

Solving structural dynamics with uncertainty quantification via evidential neural operators

Pei-Lin Li^{1, 2, 3}, 0009-0007-6195-6435, Yi-Qing Ni^{1, 2}, 0000-0003-1527-7777, Jian-Ming Ling³, Shi-Fu Liu³, You-Wu Wang^{1, 2}, 0000-0003-2293-4712

¹Department of Civil and Environmental Engineering, The Hong Kong Polytechnic University, Hong Kong Special Administrative Region of China

²National Rail Transit Electrification and Automation Engineering Technology Research Center (Hong Kong Branch), Hung Hom, Kowloon, Hong Kong Special Administrative Region of China

³The Key Laboratory of Road and Traffic Engineering, Ministry of Education, Tongji University, Shanghai, 201804, China
email: peilin.li@connect.polyu.hk, ceyqni@polyu.edu.hk, jmling@tongji.edu.cn, sflu@tongji.edu.cn, youwu.wang@polyu.edu.hk

ABSTRACT: Solving structural dynamic equations is crucial for evaluating the reliability and safety of civil infrastructures such as bridges, airport runways and railways under various loads. Currently, the Neural Operator (NO) shows great potential in solving structural dynamic equations under various excitations and boundary conditions without retraining and are capable of zero-shot learning. However, there has been a dearth of research into providing prediction errors and explicit uncertainty quantification of the operator-learned model for computing structural responses in different data regimes. This research aims to approximate the solution operator of structural dynamic equations with uncertainty quantification. Deep evidential learning is introduced to establish the Evidential Neural Operator (ENO) and the epistemic uncertainty of structural responses can be obtained. An illustrative example is given in this paper, which shows that the E-NO model can effectively identify the well-prediction condition and the worse-prediction condition. This work can provide an end-to-end framework for building surrogate models of real-world structures, which can rapidly compute structural responses with uncertainty.

KEYWORDS: Structural Dynamics; Uncertainty Quantification; Evidential Deep Learning; Neural Operator.

1 INTRODUCTION

The uncertainty analysis of structural systems is the key to ensuring the safety and reliability of structural design. The conventional physical model-based method can analyze the uncertainty of the forward computation under random material parameters, geometric dimensions or external excitation through the probabilistic or non-probabilistic framework [1]. Probabilistic uncertainty analysis methods such as Monte Carlo simulation [2], [3], stochastic finite element method [4], [5], etc., statistically sample uncertainty propagation on uncertainty parameters by calculating models or conducting experiments. Non-probabilistic methods such as interval analysis [6], [7] and fuzzy theory [8], [9], which are different from probabilistic methods, are suitable for analyzing the epistemic uncertainty caused by a lack of knowledge in the absence of deterministic prior information. The above methods are versatile and flexible in the form of the model, but the calculation cost would greatly increase to conduct the uncertainty analysis of large-scale and high-dimensional structures.

With the breakthrough of deep learning technology, neural operators [10], [11] can effectively learn the global mapping relationship of complex systems, especially for the cross-resolution solution of high-dimensional and nonlinear problems, which reduces the computational cost compared with traditional physical modeling methods. Chawit et al. established the vehicle-bridge interactive neural operator as a surrogate model of the bridge structure, which can more accurately predict the structural response under different structural damage fields than the traditional finite element model [12]. Ding et al. solved the coupled differential equations of structural dynamics based on the physics-informed neural operator (PINO-CDE). Also, PINO-CDE provides a higher resolution for uncertain propagation tasks, which takes less

than a quarter of the computing time compared to the probability density evolution method [13].

However, the neural operator mapping process is nonlinear and non-intuitive. The results are affected by multiple sources of uncertainty, such as aleatoric uncertainty and epistemic uncertainty [14], [15]. Most of the existing studies focus on the probability distribution of the output results of neural operators, but it is difficult to distinguish the sources of quantitative uncertainty. This fuzziness may lead to misjudgment in practical engineering based on computing results. While deep evidential learning provides a feasible path for aleatoric and epistemic uncertainty qualification of regression problems [16]. Therefore, how to integrate deep evidential learning and neural operators to build an efficient and interpretable computational uncertainty framework for dynamic structures is worth exploring.

In this work, we propose an evidential neural operator, extending evidential deep learning to a more flexible and complex neural network like the Fourier neural operator. For parametric structural dynamic systems with stochastic structural parameters and load excitation, ENO can quantitatively distinguish aleatoric uncertainty and epistemic uncertainty in the forward computation without retraining. The multi-task regularizer is introduced in ENO to improve adaptability to high-dimensional scenarios and complex structural systems, by flexibly controlling the weights of regularizer. A single-degree-of-freedom system is provided as a numerical example to verify the accuracy of uncertainty estimation and quantization distinction.

2 THEORETICAL BASIS

2.1 Fourier Neural Operator

Fourier Neural Operator (FNO) can capture high-frequency characteristics of dynamic systems by Fast Fourier Transform

and spectrum convolution operation and is suitable for solving structural vibration differential equations to simulate the dynamic behavior of structural systems.

Besides, performing convolution in Fourier space greatly reduces the computational complexity. For a single hidden layer (1), the Fourier neural operator utilize the kernel-integral operator, extend deep neural networks to infinite dimensions:

$$(N_l V)(x) = \sigma(A_l V(x) + B_l(x) + \int_D K_l(x, y) V(y) dy) \quad (1)$$

Due to,

$$K_l(x, y) = K_l(x - y) \quad (2)$$

$$\int_D K_l(x - y) V(y) dy = K_l \times V \quad (3)$$

Using the Fourier transform result in (4):

$$K_l \times V = f^{-1}(f(K) \cdot f(V)) \quad (4)$$

Hence, the computational complexity can be reduced from $O(N^2)$ to $O(N \log(N))$. FNO shows great potential for fast and accurate computation of oscillatory differential equations.

2.2 Evidential Neural Operator

The sources of uncertainty can be divided into aleatoric uncertainty and epistemic uncertainty. Evidential theory assumes that the prediction target Z_i can be independently sampled from the Gaussian distribution. Then, a probabilistic estimate of its mean and variance is required.

The normal-inverse-gamma (NIG) prior distribution is introduced in evidential regression [16]. The mean μ is assumed to follow a Gaussian distribution, and the variance σ is assumed to follow an inverse gamma distribution. By marginalizing μ and σ , the model evidence can be expressed as a Student-t distribution (5):

$$p(z_i | \theta) = St(z_i; \gamma, \frac{(1+\tau)\beta}{\tau\alpha}, 2\alpha) \quad (5)$$

where θ represents the combination of parameters of the NIG distribution. γ represents the expectation of the mean μ . τ is the precision parameter of the Gaussian distribution. α and β are the shape parameters of the inverse gamma distribution.

Combining the high-dimensional computing capability of FNO and the ability of NIG high-order distribution for capturing data diversity and uncertainty. The evidential neural operator is proposed to convert the model output into four parameters of NIG distribution. The loss function (6) of the evidential neural operator is designed for uncertainty sources, which can be divided into two parts: negative log-likelihood loss and evidence regularizer.

$$\mathcal{L}_{ENO} = \mathcal{L}_{NLL} + \sum_{i=1}^n \lambda_i \mathcal{L}_{REGi} \quad (6)$$

where,

$$\mathcal{L}_{NLL} = \frac{1}{2} \log\left(\frac{\pi}{\tau}\right) - \alpha \log(\phi) + \left(\alpha + \frac{1}{2}\right) \log((z_i - \gamma)^2 \tau + \phi) + \log\left(\frac{\Gamma(\alpha)}{\Gamma(\alpha + \frac{1}{2})}\right)$$

$$\mathcal{L}_{REGi} = |z_i - \gamma| \cdot (2\tau + \alpha)$$

where, $\phi = 2\beta(2\tau + \alpha)$. n represents the number of regularizers for different outputs.

In this work, ENO adds multi-task regularization to ensure that each task has independent error and evidence constraints, and can better adapt to multi-task learning and complex scenarios by flexibly controlling regularization weights. The data normalization module is incorporated into the training process to normalize and denormalize the dataset to address the potential training instability and gradient explosions arising from differences in the scale of output variables.

3 ILLUSTRATIVE EXAMPLE

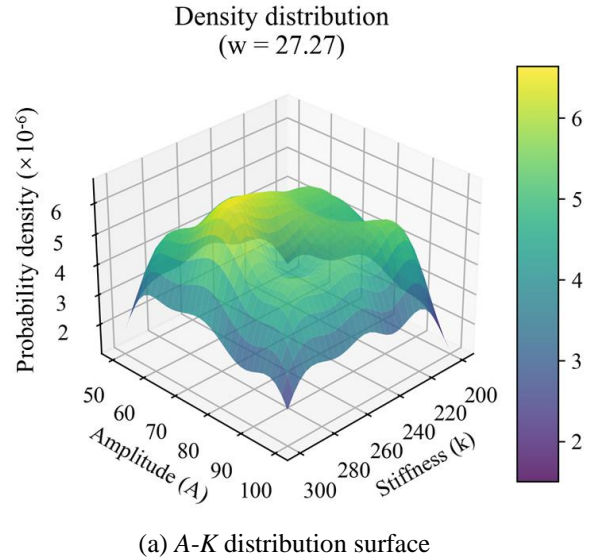
For validating the effectiveness of ENO, a single degree of freedom random vibration equation (7) with harmonic excitation is used as an example to solve the forward uncertainty of response prediction:

$$M\ddot{u} + C\dot{u} + Ku = A \sin(wt) \quad (7)$$

where, M is mass, $M = 1\text{kg}$. C is damping and K is stiffness. A represents amplitude and w represents the frequency of the harmonic force. u , \dot{u} , \ddot{u} represent the displacement, velocity, and acceleration, respectively.

K , A , and w are randomly sampled with a uniform distribution. The sampling interval of stiffness is $[200, 300]$ N/m. The sampling interval of amplitude and frequency are $[50, 100]$ N and $[10, 45]$ rad/s, respectively. The probability density surface diagrams of three stochastic variables are shown in Figure 1. The Newmark- β integral algorithm is used to solve equation (7) and generate the datasets. The proportions of the training set, verification set and test set are 70%, 20% and 10%, respectively. The network parameters, such as convolutional layer depth D_{conv} , convolutional layer width W_{conv} , fully connected layer depth D_{fc} and width W_{fc} of FNO were optimized by using the Bayesian optimization algorithm. The optimal network parameters were determined as follows: $D_{\text{conv}}=4$, $W_{\text{conv}}=32$, $D_{\text{fc}}=3$, and $W_{\text{fc}}=64$.

The ENO model is implemented in PyTorch and the Fourier modes of spectral convolution layers are 26. The weight parameters of the loss item are: $\lambda_1 = 1$, $\lambda_2 = 2$, $\lambda_3 = 2$. The total number of epochs is 300 and the Adam optimizer was used with a learning rate of 10^{-3} .



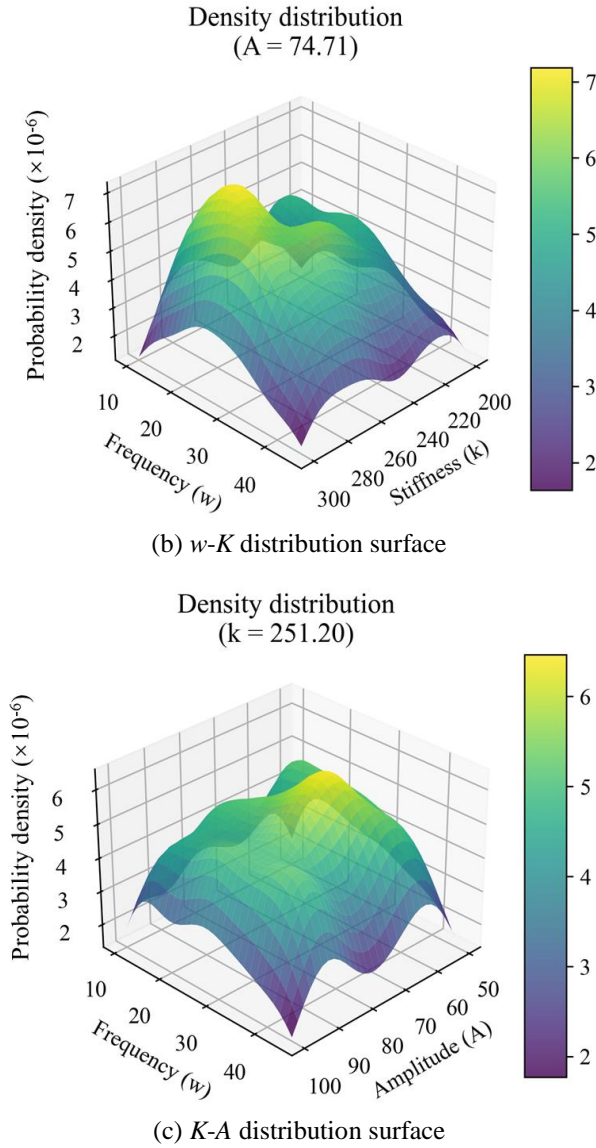


Figure 1. Probability density surfaces of stochastic variables.

The ENO model is validated against the state-of-the-art Deep Ensemble model presented in [17]. The baseline model is also embedded in the FNO framework (FNO-DE) to conduct ablation experiments, and the network parameters are consistent with those adopted by ENO. FNO-DE consists of five independently trained models with identical architecture but different random initializations. The evaluation metrics applied Root Mean Square Error (RMSE), Empirical Coverage Probability (ECP) and Pearson Correlation Coefficient (R_{pr}). RMSE can evaluate the error level between the predicted mean and the ground truth. ECP monitors the proportion of samples falling into the predicted confidence interval to the total number of samples. In this work, 95% confidence is considered, and the ideal value of ECP should be close to 0.95. Besides, the Pearson Correlation Coefficient can evaluate the correlation between prediction error and uncertainty.

4 RESULTS AND DISCUSSION

For solving the single-degree-of-freedom vibration equation, the ENO model performance was first tested by sampling test sets in the interval. The outputs of displacement, velocity and

acceleration responses and their corresponding uncertainties are shown in Figure 2. Due to the high cognition level of the tested model within the interval, it can be seen that the aleatoric and epistemic uncertainty are both small, which are lower than 10^1 .

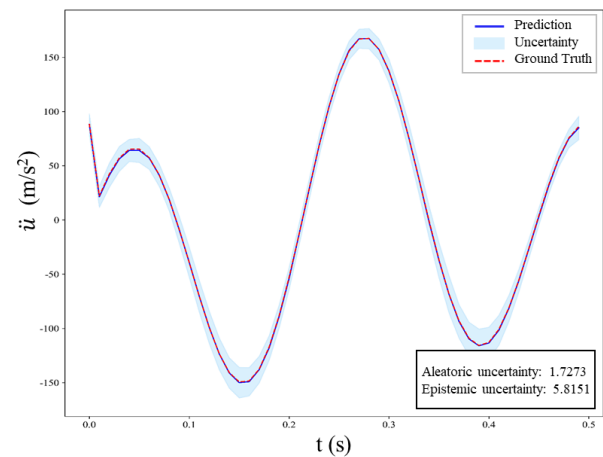
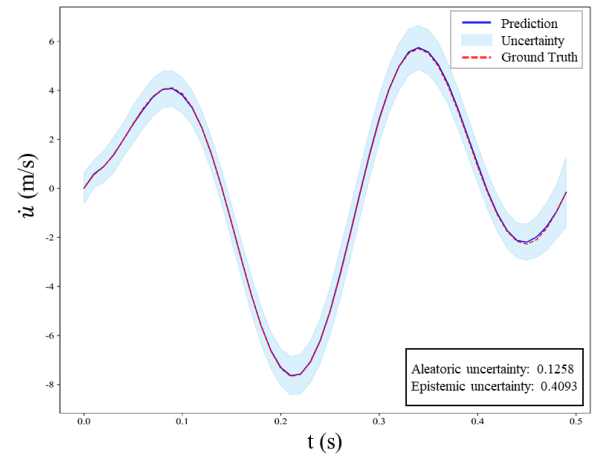
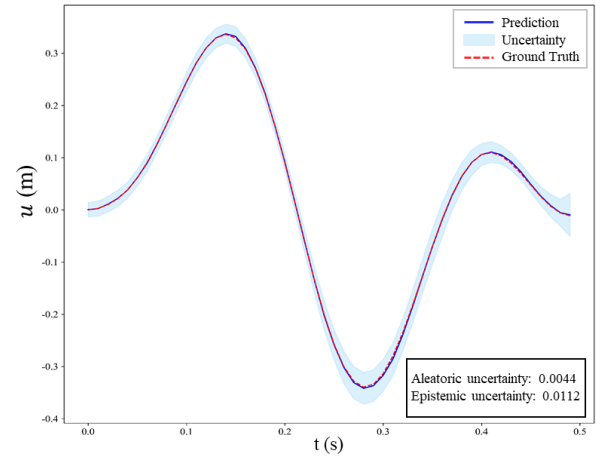
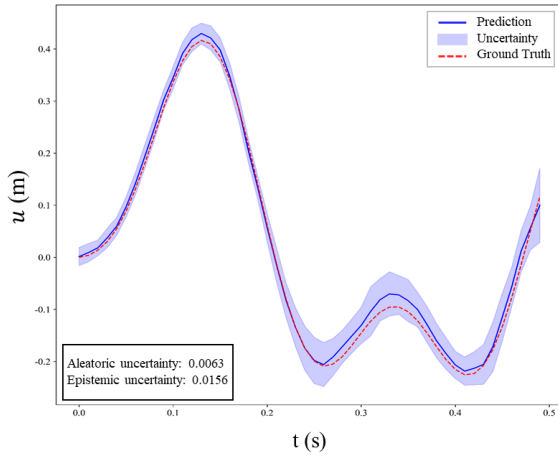


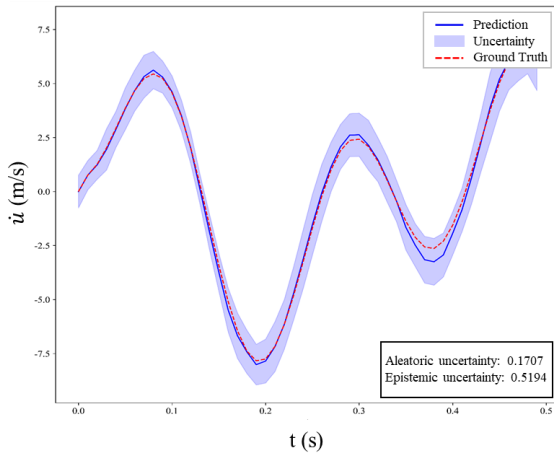
Figure 2. Uncertainty prediction in the distribution (ENO).

The out-of-distribution test evaluates the zero-shot learning ability and generalization of the ENO model. The results of out-of-interval testing are shown in Figure 3. The epistemic

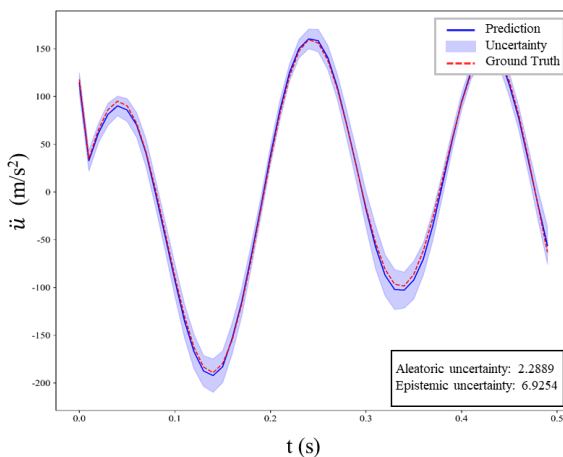
uncertainty of the model has increased by 20~40%, compared with that in distribution testing. And the epistemic uncertainty is always greater than the aleatoric uncertainty of the raw data, due to no extra noise added in the dataset for this illustrative case.



(a) Uncertainty prediction of the displacement



(b) Uncertainty prediction of the velocity



(c) Uncertainty prediction of the acceleration

Figure 3. Uncertainty prediction out of distribution (ENO).

The performance comparison between the ENO model and the FNO-DE model is shown in Table 1. The ENO model can achieve higher fitting accuracy than the FNO-DE model. The RMSE of ENO is less than that of FNO-DE, especially when

ENO is tested out of distribution. ENO has better generalization performance. In terms of uncertainty prediction, FNO-DE remains competitive in in-distribution testing, and the empirical coverage probability of both ENO and FNO-DE is relatively close to the nominal values. However, the uncertainty estimated by ENO shows a stronger correlation with prediction errors ($R_{pr} \sim 0.86$) in interpreting out-of-domain data.

Table 1. Compared the metrics of ENO and FNO-DE models.

In distribution			Out of distribution		
Metrics	ENO	FNO-DE	Metrics	ENO	FNO-DE
RMSE	0.35	0.38	RMSE	2.22	2.41
ECP	1.0	1.0	ECP	1.0	0.82
R_{pr}	0.70	0.79	R_{pr}	0.86	0.67

5 CONCLUSION

In this paper, a novel evidential neural operator is proposed, which cooperates with the basic principle of deep evidential learning and the high-dimensional nonlinear mapping capability of the Fourier neural operator. ENO provides a scientific machine learning framework for the uncertainty quantification for the forward computation of structural vibration equations. This work solves the vibration equation of a single degree of freedom as a numerical example, indicating that the model has higher epistemic uncertainty when tested outside the interval. Compared to the evaluating metrics with the art-of-state ensemble model, the ENO shows superior uncertainty calibration and fitting accuracy in out-of-domain testing. Future works would consider the effect of data noise on the uncertainty qualification and expand the ENO to a more complex structural system.

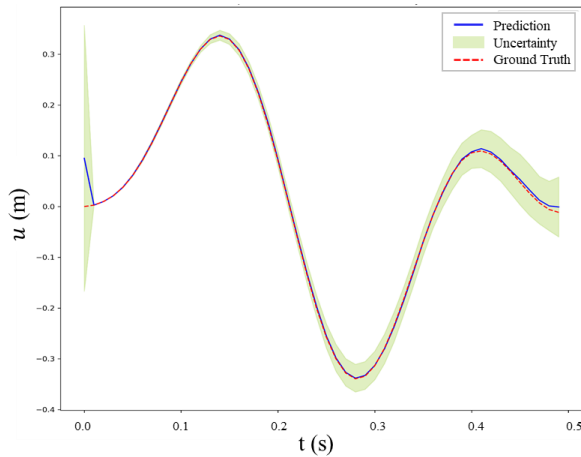
ACKNOWLEDGMENTS

The work described in this paper was supported by a grant from the Research Grants Council (RGC) of the Hong Kong Special Administrative Region (SAR), China (Grant No. PolyU 152308/22E) and a grant from The Hong Kong Polytechnic University (Grant No. 1-WZ0C). The authors would also like to appreciate the funding support by the Innovation and Technology Commission of Hong Kong SAR Government to the Hong Kong Branch of National Rail Transit Electrification and Automation Engineering Technology Research Center (Grant No. K-BBY1).

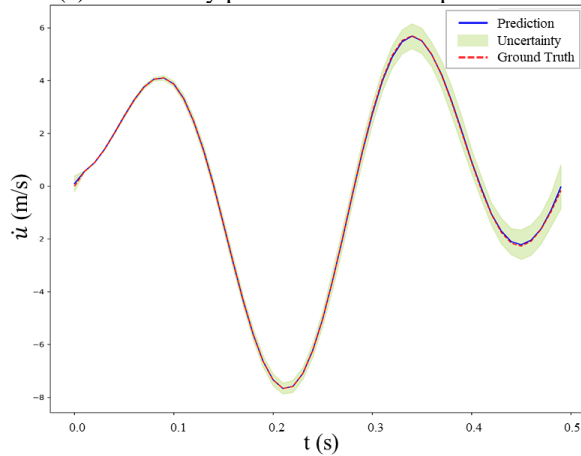
APPENDIX: PREDICTION RESULTS OF FNO-DE

A-1: Test results of FNO-DE within the interval

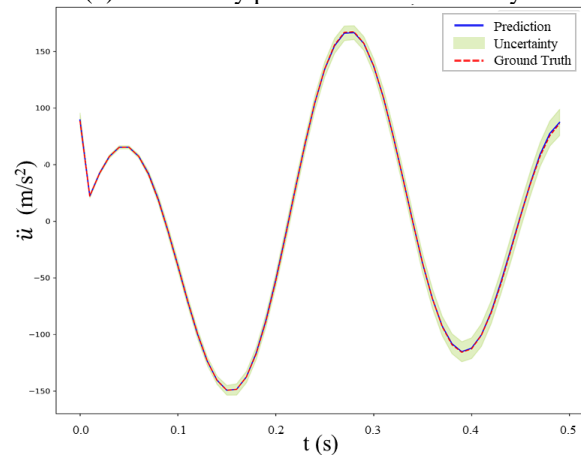
The test results of the baseline model (FNO-DE) within the sampling interval are also shown in Figure 4. The predicted responses are generally consistent with the ground truth, indicating the FNO-DE can capture the dynamic change trend of the displacement and its derivative. The regions with large uncertainties are mainly concentrated at the boundaries of time, such as around $t = 0$ and $t \approx 0.5$, while the uncertainty distribution is narrow within the time interval. This demonstrates that the FNO-DE model is quite sensitive and can not comply well with the boundary conditions.



(a) Uncertainty prediction of the displacement



(b) Uncertainty prediction of the velocity

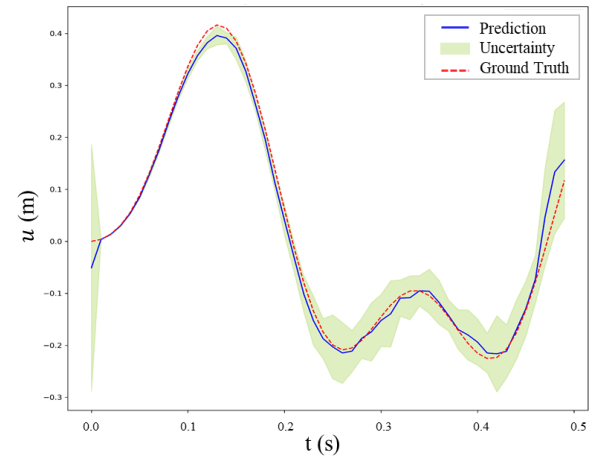


(c) Uncertainty prediction of the acceleration

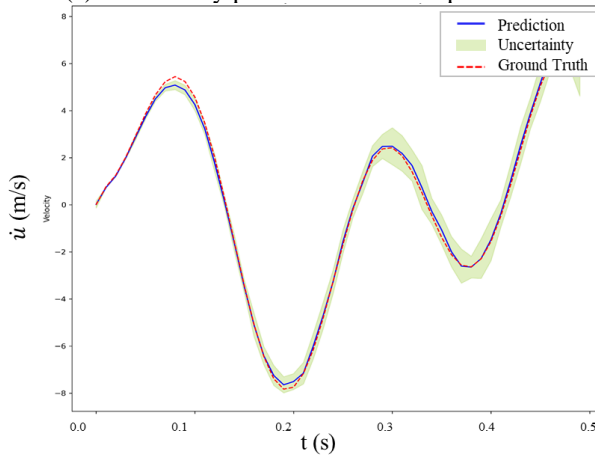
Figure 4. Uncertainty prediction in the distribution (FNO-DE).

A-2: Test results of FNO-DE out of the interval

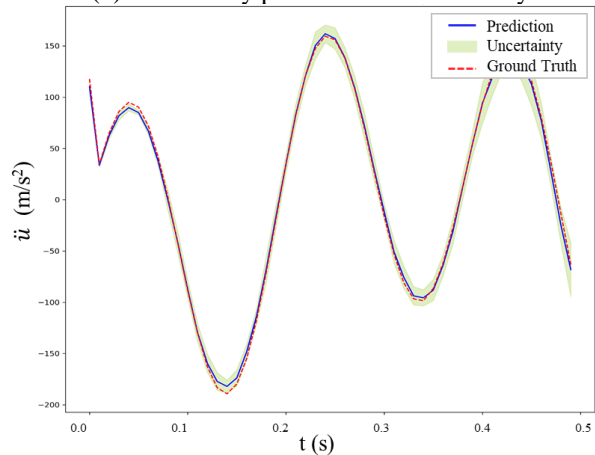
Outside the sampling interval (Figure 5), the deviation between the model prediction results and the Ground Truth increases, while the uncertainty region (green shadow) expands significantly, especially around the time period $t = 0.4s$, where the confidence interval of displacement $u(t)$ increases from about ± 0.1 m to ± 0.2 m. This shows that the prediction confidence of FNO-DE for unseen data is greatly reduced.



(a) Uncertainty prediction of the displacement



(b) Uncertainty prediction of the velocity



(c) Uncertainty prediction of the acceleration

Figure 5. Uncertainty prediction out of the distribution (FNO-DE).

REFERENCES

- [1] K. Zhou, Z. Wang, Q. Gao, et al, Recent advances in uncertainty quantification in structural response characterization and system identification, Probabilistic Engineering Mechanics, 2023, 74, 103507.
- [2] C. Z. Mooney, Monte carlo simulation (No. 116), Sage, 1997.
- [3] P. Marek, J. Brozzetti, M. Gustar, et al, Probabilistic assessment of structures using Monte Carlo simulations, Applied Mechanics Reviews, 2002, 55(2), B31-B32.
- [4] S. Naskar, T. Mukhopadhyay, S. Sriramula, et al, Stochastic natural frequency analysis of damaged thin-walled laminated composite beams

- with uncertainty in micromechanical properties, *Composite Structures*, 2017, 160, 312-334.
- [5] H. Zhang, N. An, X. Zhu, Structural dynamic reliability analysis of super large-scale lattice domes during earthquakes using the stochastic finite element method, *Soil Dynamics and Earthquake Engineering*, 2022, 153, 107076.
- [6] M. Modares and R. L. Mullen, Dynamic analysis of structures with interval uncertainty, *Journal of Engineering Mechanics*, 2014, 140(4), 04013011.
- [7] K. Shariatmadar and M. Versteyhe, Numerical linear programming under non-probabilistic uncertainty models—interval and fuzzy sets, *International Journal of Uncertainty, Fuzziness and Knowledge-Based Systems*, 2020, 28(03), 469-495.
- [8] C. Wang and H. G. Matthies, Coupled fuzzy-interval model and method for structural response analysis with non-probabilistic hybrid uncertainties, *Fuzzy Sets and Systems*, 2021, 417, 171-189.
- [9] Z. Ni and Z. Qiu, Hybrid probabilistic fuzzy and non-probabilistic model of structural reliability, *Computers & Industrial Engineering*, 2010, 58(3), 463-467.
- [10] N. Kovachki, Z. Li, B. Liu, et al, Neural operator: Learning maps between function spaces with applications to pdes, *Journal of Machine Learning Research*, 2023, 24(89), 1-97.
- [11] Z. Li, N. Kovachki, K. Azizzadenesheli, et al, Fourier Neural Operator for Parametric Partial Differential Equations, In *International Conference on Learning Representations*, 2020.
- [12] C. Kaewnurachadasorn, J. Wang, C. W. Kim, Neural operator for structural simulation and bridge health monitoring, *Computer-Aided Civil and Infrastructure Engineering*, 2024, 39(6), 872-890.
- [13] W. Ding, Q. He, H. Tong, et al, Solving coupled differential equation groups using PINO-CDE, *Mechanical Systems and Signal Processing*, 2024, 208, 111014.
- [14] A. Der Kiureghian and O. Ditlevsen, Aleatory or epistemic? Does it matter?, *Structural safety*, 2009, 31(2), 105-112.
- [15] E. Hofer, M. Kloos, B. Krzykacz-Hausmann, et al, An approximate epistemic uncertainty analysis approach in the presence of epistemic and aleatory uncertainties, *Reliability Engineering & System Safety*, 2002, 77(3), 229-238.
- [16] A. Amini, W. Schwarting, A. Soleimany, et al, Deep evidential regression, *Advances in neural information processing systems*, 2020, 33, 14927-14937.
- [17] B. Lakshminarayanan, A. Pritzel, C. Blundell, Simple and scalable predictive uncertainty estimation using deep ensembles, *Advances in neural information processing systems*, 2017, 30.